HIGH PERFORMANCE CREEP RESISTANT STEELS FOR 21st CENTURY POWER PLANTS

Fujio Abe - National Institute for Materials Science (NIMS), Japan

ABSTRACT

Research and development of heat resistant steels and alloys for high-efficient power plants at 650°C and above are being now promoted in Europe, USA and Japan. Great advancement has been achieved in the analysis of specific microstructure instability causing a loss of creep strength, the prediction of onset time of the creep strength loss and the theoretical modelling of precipitation sequences in power plant steels. A number of highly creep-resistant martensitic 9Cr steels with higher creep rupture strength than existing high strength steels such as T91 and P92 have been proposed at NIMS project in Japan for application to 650°C USC plants. The formation of thin scale of Cr-rich oxides is achieved on the surface of 9Cr steel by the combination of Si addition and pre-oxidation treatment in argon gas at 700°C. This significantly improves oxidation resistance of 9Cr steel in steam at 650°C. The addition of boron suppresses the Type IV fracture in HAZ at low stresses and significantly improves the creep rupture strength of welded joints. Approximately no difference in microstructure between HAZ and base metal produces no mechanical constrain effect in HAZ. The future prospect of austenitic steels for 700°C USC plants is also described.

KEYWORDS

9Cr steel, creep strength, MX carbonitride, $M_{23}C_6$ carbide, Z-phase, Laves phase, boron, oxidation, Cr oxide scale, welded joint, Type IV fracture, austenitic steel

INTRODUCTION

Energy security combined with lower carbon dioxide emissions is increasingly quoted to protect global environment in the 21st century. Coal provides us abundant, low cost resources for electric power generation. In China and India, electric power generation by coal-fired power plants becomes highly increased to meet the needs of growing population and economy. However, traditional coal-fired power plants emit environmentally damaging gases such as CO_2, NO_x and SO_x at high levels relative to other electric power generation options. Adoption of ultra supercritical (USC) power plants with increased steam parameters significantly improves efficiency, which reduces fuel consumption and the emissions of environmentally damaging gases. For example, the increase in steam parameters from conventional 536/566°C and 24.1 MPa to 650/593/593°C and 34.3 MPa causes an increase in relative efficiency of 6.5%, which results in significant coal saving and hence the reduction of CO_2 emissions [1].

Kern et al. [2] showed that recently a continuous increase in steam parameters can be observed worldwide as shown in **Figure 1**. In Japan, coal-fired steam power plants have been already extending to USC conditions. Today, China seems to be adopting the new technologies to use USC conditions for the challenge of developing their electricity supply industry. They also pointed out that natural gas plays an important role in the present energy market situation but that beside land-based gas turbines, coal-fired power plants operated with steam will also play an important role in the future. The largest and the most reliable fossil energy resources in the future seem to be coal around the world.

The increase in steam parameters above 600°C requires extensive R&D of advanced ferritic/martensitic steels with sufficient long-term creep rupture strength higher than conventional

ones. At present, national and international projects aiming at the development of high-Cr martensitic steels capable of steam conditions up to 650°C are being promoted at NIMS [3] in Japan and at COST536 program [2, 4] in Europe. In addition to enough creep strength, high operational flexibility is another issue for thick section components in USC plants. 9-12Cr martensitic steels can offer the highest potential to meet the required flexibility, because of their smaller thermal expansion and larger thermal conductivity than austenitic steels and Ni base superalloys.

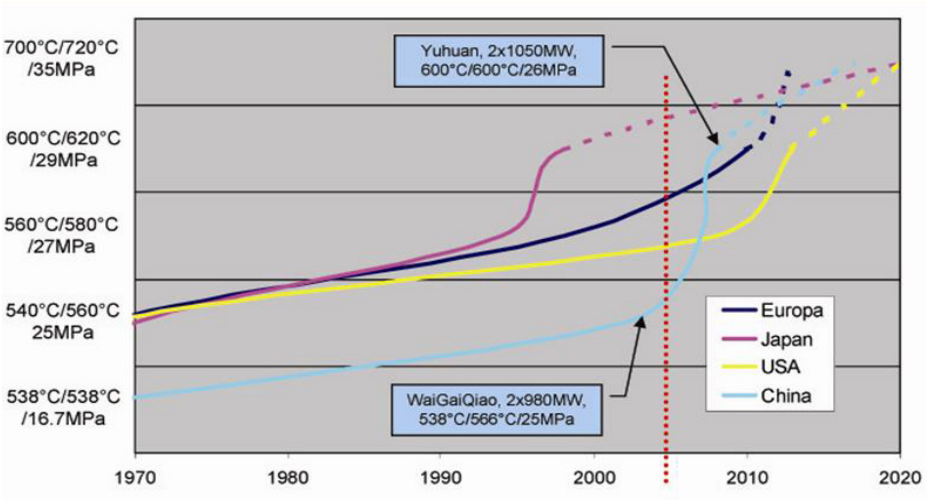

Figure 1 Improvement of steam parameters in Europe, Japan, USA and China [2]

Further advanced steam conditions of 700°C and above have been already initiated to gain net efficiency higher than 50% at Thermie AD700 project [5] aiming at 700°C in Europe and at DOE Vision 21 project [6] aiming initially at 760°C but recently modified at 732°C in the US. These projects involve the replacement of 9-12Cr martensitic steels by nickel base superalloys for the highest temperature components. It should be noted that nickel base superalloys are much more expensive than ferritic/martensitic steels. To minimize the requirement of expensive nickel base superalloys, 9-12Cr martensitic steels can be applied to the next highest temperature components of such very high temperature plants. Therefore, 9-12Cr martensitic steels are strongly desired to expand the present temperature range up to 650°C and more.
This paper describes recent advances in 9-12Cr martensitic steels for 650°C USC plant and the future prospect. The present status of austenitic steel development is also described, because austenitic steels are being considered as one of candidates for 700°C USC plants in Japan.

RECENT ADVANCES IN 9-12Cr MARTENSITIC STEELS

*Loss of creep rupture strength at long times and prediction of degradation behavior**

The loss of creep rupture strength has extensively been investigated for a number of 9 to 12 Cr steels [7]. The proposed mechanisms are due to the occurrence of microstructure degradation during creep exposure and are classified as (a) dissolution of fine M_2X and MX carbonitrides and

---

** The sections with asterisk are based on a review paper by the present author [7]. Detailed references are given in ref. [7].*

precipitation of new phases, (b) preferential recovery of microstructure in the vicinity of prior austenite grain boundaries, (c) loss of creep ductility and (d) recovery of excess dislocations. The precipitation of Z-phase, M_6X carbonitrides and $Fe_2(W,Mo)$ Laves phase during creep causes a loss

of creep strength at long times, because they consume existing fine M_2X and MX and or $M_{23}C_6$ precipitates. Z-phase is a complex nitride of the form Cr(Nb,V)N. **Figure 2** shows the sigmoidal behavior in creep rupture data for 0.1C-0.55Mn-0.07Si-10.84Cr-0.14Mo-2.63W-2.86Co-0.55Ni-0.19V-0.06Nb-0.016N-0.019B steel (TAF 650) at 650°C, comparing with the data for original TAF and Mod.9Cr-1Mo (T91) [8] and the formation of Z-phase [9]. The synergetic effect of Z-phase precipitation and tungsten depletion of solid solution due to Fe_2W Laves phase formation could be the reason for the sigmoidal shape of creep rupture strength curve of TAF 650 steel.

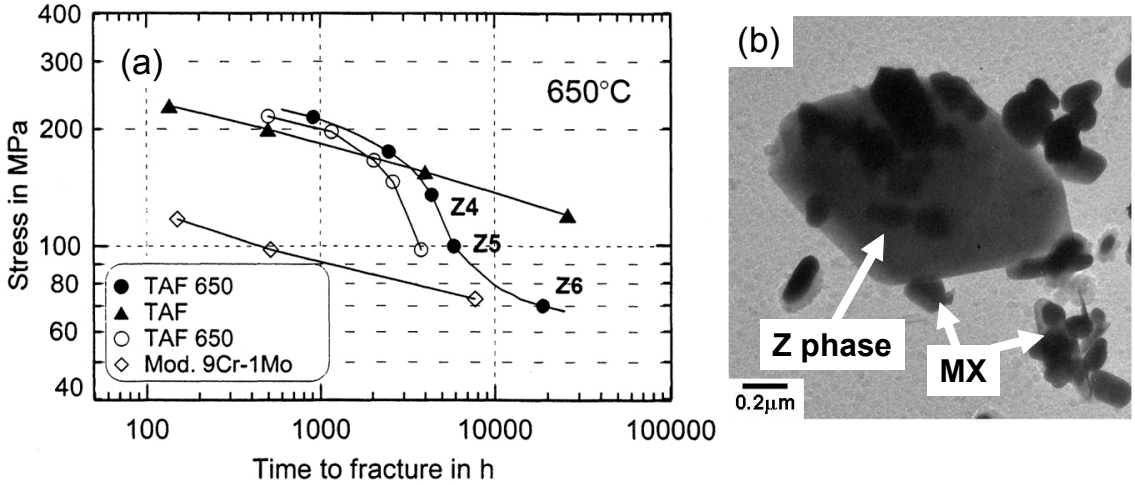

Figure 2 (a) Comparison of stress versus time to rupture curves for various martensitic steels at 650°C [8] and (b) formation of Z-phase in NF12 [9].

The loss of creep rupture strength in T91 steel is reported to be due to preferential recovery of the microstructure in the vicinity of prior-austenite grain boundaries, as shown in **Figure 3** [10]. The referential recovery promotes the onset of acceleration creep and hence causes premature rupture. The dissolution of MX and the precipitation of Z-phase promote the preferential recovery.

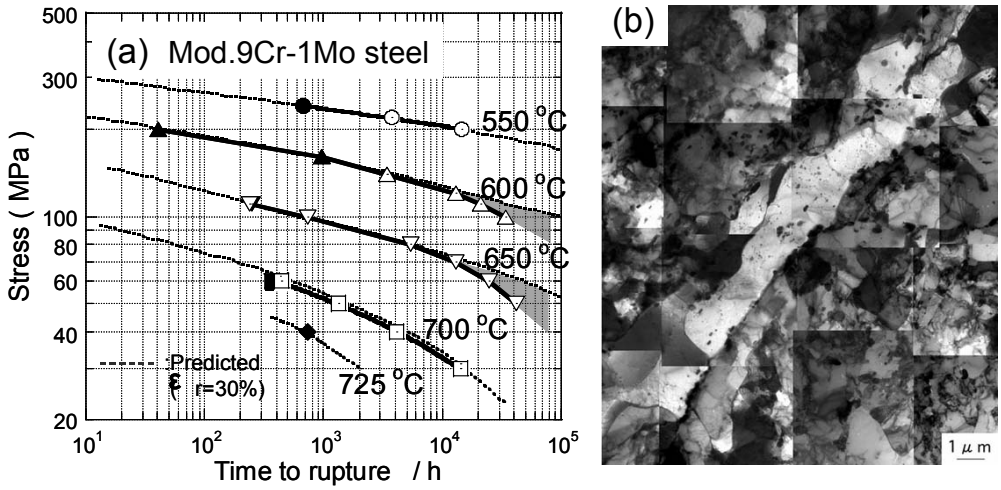

Figure 3 (a) Stress versus time to rupture curves for Mod.9Cr-1Mo steel (T91) and (b) TEM micrograph after creep rupture testing for 34,141 h at 600oC and 100MPa [10].

Strang et al. [11] investigated parametric extrapolation for the prediction of long-term creep rupture strength of 9 to 12Cr power plant steels, such as 9Cr1Mo(V), 12CrMoVNbN, X19CrMoVNbN and TAF650, taking the sigmoidal behavior into account. Analysis of the data using the Manson parameter showed a temperature dependency on both the stress and duration of the sigmoidal

inflection point. However, the effect of testing temperature on the sigmoidal inflexion stresses is very small being only between 1-2 %, which is much smaller than actual values.
Maruyama et al. [12] pointed out that fracture mechanisms often changed from ductile transgranular fracture at shorter life (high stress) to brittle fracture at longer life (low stress) and that the change in fracture mechanisms made a difficulty in evaluating long term rupture life. He proposed a new method based on multiple region analysis taking different fracture modes into account for evaluating long term creep rupture strength. On the other hand, Kimura et al. [13] reported that the inflection in a number of steels, including T91 steel, took place at the stress condition corresponding to half of 0.2% proof stress at the testing temperature. Half of 0.2% proof stress was almost the same as elastic limit at the testing temperature. The creep rupture strength of T91 steel at 10^5 h was adequately evaluated by Larson-Miller parameter with the selected data under the stresses lower than half of 0.2% proof stress.

Microstructure evolution during exposure at elevated temperature*

In martensitic 9 to 12Cr steels, efforts have been paid to the precipitation behavior of Z-phase, M_6X and $Fe_2(Mo,W)$ Laves phase and the stability of MX and $M_{23}C_6$ during creep exposure, because they cause a loss of long-term creep strength [7]. The coarsening of $M_{23}C_6$ carbides in 12CrMo(W)VNbN steels is accompanied by dissolution of fine MX carbonitrides due to the precipitation of coarse M_6X and or Z-phase. Increase in Ni content in 12CrMoV steel results in accelerated microstructure degradation with more rapid coarsening of $M_{23}C_6$, dissolution of MX, precipitation of coarse M_6X and Fe_2Mo. The formation of coarse Z-phase is also observed in T91 steel at 600 and 650^{o}C. Increase in nitrogen content results in accelerated microstructure degradation during creep at 650^{o}C with more rapid precipitation of Z-phase.
Re-dissolution of vanadium nitrides and two-phase separation of primary MX carbonitrides are demonstrated for high-Cr steels during heat treatment. Energy filtering transmission electron microscopy allows a reliable quantitative distinction between $M_{23}C_6$, VN and Laves phases to establish size distribution of these precipitates in different specimen conditions. Atom probe field ion microscopy measurement shows that boron is incorporated and evenly distributed within $M_{23}C_6$, M_6C, MX and Laves phases in power plant steels and that boron is not segregated to the precipitate-matrix interface. Scanning Auger spectroscopy shows that the enrichment of boron in $M_{23}C_6$ carbides is more significant in the vicinity of prior austenite grain boundaries than in the matrix far from grain boundaries. The effects of microstructure evolution on creep strength have extensively been investigated for a number of power plant steels with emphasis on long-term behavior.

Modelling of precipitation sequence and theoretical design of creep-resistant steels*

Bhadeshia and his co-workers [14] have established a new model for multiple precipitation reactions, which includes multicomponent treatments of both diffusion-controlled growth and capillarity. The new model shows good agreement with experimental data about not only volume fractions but also particle sizes for each alloy carbide in 3Cr-1.5Mo and 2.25Cr-1Mo steels. Murata et al. [15] have successfully applied the concept of system free energy to the prediction of formation and morphological change of Fe_2W Laves phase in Fe-10Cr-W-C quaternary steels. A phenomenological calculation based on cluster variation method has been attempted to seek inexpensive substituting elements for Pd in fine precipitates of FePd-$L1_0$ intermetallic compound in 9Cr steel and to calculate phase equilibria for $FeNi_3$ and FeNi phases in 9Cr steel [16].
A neural network model has been combined with thermodynamic and kinetic calculations, together with metallurgical experience, to propose two alloys, steel A and steel B, with stress rupture properties which are predicted to be better than existing 10CrMoW steel [17]. The chemical compositions are 0.12C-0.48Mn-9Cr-0.75Mo-3W-1.25Co-0.21V-0.01Nb-0.064N-0.008B-0.0003Ta-0.0003Re (steel A) and 0.13C-0.5Mn-8.7Cr-0.3Mo-3W-0.21V-0.01Nb-0.064N-0.008B-

0.0003Ta-0.0003Re (steel B). Comparing with existing 10CrMoW steel, there is reductions in the Mn and Cr concentrations together with an increase in the level of W. The experimental results on creep rupture strength of the alloy-designed steels have not been reported.

Development of 9-12Cr martensitic creep-resistant steels for 650°C USC plant*

Figure 4 shows the creep rupture data for high strength martensitic 9 to 12Cr steels at 650°C [7]. In this figure, two 9Cr-3W-3Co-0.2V-0.05Nb steels with 0.05N-0.002C (0.002C steel [18]) and with 0.08C-0.0139B (0.0139B steel [19]) are experimental steels developed by NIMS, Japan, 12Cr-2.6W-2.5Co-0.5Ni-0.2V-0.05Ni steel (NF12) and 12Cr-3W-3Co-0.2V-0.05Nb-0.1Ta-0.1Nd-0.05N steel (SAVE12) are experimental steels developed by Japanese steelmaking companies as upgrade versions of P92 and P122, respectively, and oxide dispersion strengthened (ODS) 9Cr steel [20], 0.13C-9Cr-2W-0.2Ti-0.35Y_2O_3, with martensitic microstructure is developed for fast breeder reactor cladding materials.

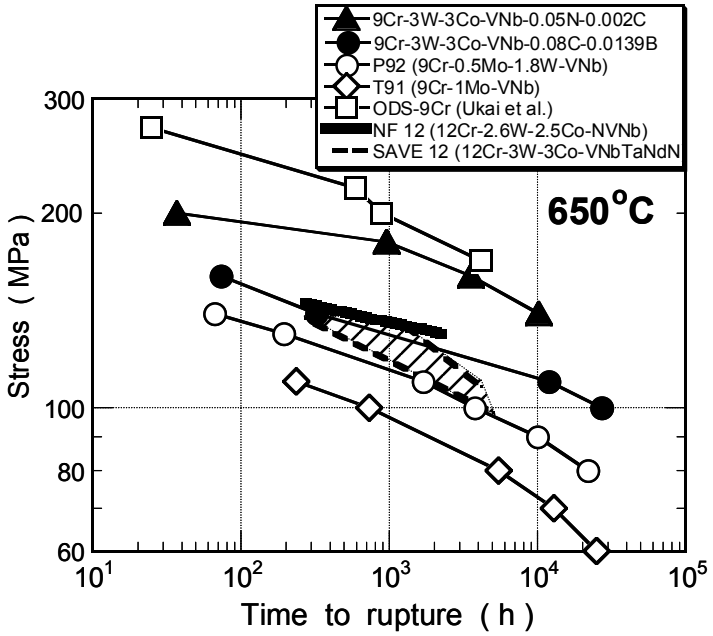

Figure 4 Creep rupture data for 0.002C and 0.0139B steels with 9Cr-3W-3Co-0.2V-0.05Nb base composition, comparing with P92, T91, NF12, SAVE12 and ODS-9Cr steels at 650°C [7]

Abe and his co-workers [21] have been exploring new alloy design concept for 9Cr steels, which is based on the stabilization of martensitic microstructure in the vicinity of prior austenite grain boundaries during creep exposure, by the addition of boron and by a dispersion of fine MX nitrides alone combined with the elimination of unstable $M_{23}C_6$ carbides for 9Cr-3W-3Co-0.2V-0.05Nb base steel. In order to maximize the effect of boron and to eliminate the formation of large boron nitrides, the addition of high boron exceeding 100 ppm was combined with no addition of nitrogen. In order to achieve a dispersion of fine MX nitrides alone, which are thermally stable particles for prolonged periods of exposure at elevated temperatures, it is crucial for 9Cr steels to reduce carbon content to very low amounts less than 50 ppm, because the addition of carbon to a 9Cr steel causes the formation of a large amount of unstable $M_{23}C_6$ carbides rich in Cr. In Fig.4, the 0.0139B and 0.002C steels, which are strengthened by boron and fine nitrides, respectively, exhibit much higher creep rupture strength than T91 and P92. The creep rupture strength of the 0.002C steel is a little bit lower than that of the ODS-9Cr steel at long times above 10^3 h, while the 0.0139B steel has approximately the same creep rupture strength as NF12 and SAVE12 at around 10^3 h. Oxide

particles are introduced by complicated mechanical alloying and therefore the production of large-scale components using the ODS-9Cr steel is not economically viable. Using Larson-Miller parameter method, the creep rupture strength at 650°C and 10^5 h is estimated to be 80 and 100 MPa for the 0.0139B and 0.002C steels, respectively. The improved creep rupture strength by the addition of boron results from the stabilization of $M_{23}C_6$ carbides in the vicinity of prior austenite grain boundaries by an enrichment of boron. The European COST-522 project has also demonstrated that a cobalt-boron containing 11Cr steel without tungsten, such as 0.17C-11Cr-1.5Mo-3Co-0.2Ni-0.2V-0.07Nb-0.01B (designated FB8), is the most favorable turbine steel for 620/630°C applications [22]. The 10^5 h creep rupture strength of the FB8 steel was estimated to be 120 and 90 MPa at 600°C and 620°C, respectively.

The minimum creep rate of the 0.002C steel in Fig.5 is much lower than that of the 0.078C steel containing similar carbon content as T91 and P92; about 1/10 at 650°C and 140MPa,as shown in **Figure 5**. This causes longer creep life in the 0.002C steel. It has been understood that the transient creep is a consequence of the movement and annihilation of excess dislocations and that the migration of lath or subgrain boundaries, causing the coarsening of lath or subgrains, is closely correlated with the onset of acceleration creep. The difference in creep rate between the two steels in the transient region is only slight as shown by 1/3 order of magnitude. The longer duration of transient creep region due to the stabilization of martensitic microstructure by pinning effect of fine MX nitrides is more effective to reduce minimum creep rate. The addition of boron to the 9Cr-3W base steel, the 0.0139B steel in Fig.4, scarcely decreases the creep rate in the transient region but it significantly retards the onset of acceleration creep and increases the duration of transient region, which effectively reduces minimum creep rate. Therefore, the stabilization of martensitic microstructure, especially near grain boundaries, is a key issue for the reduction of minimum creep rate and hence for the improvement of creep rupture strength at 650°C.

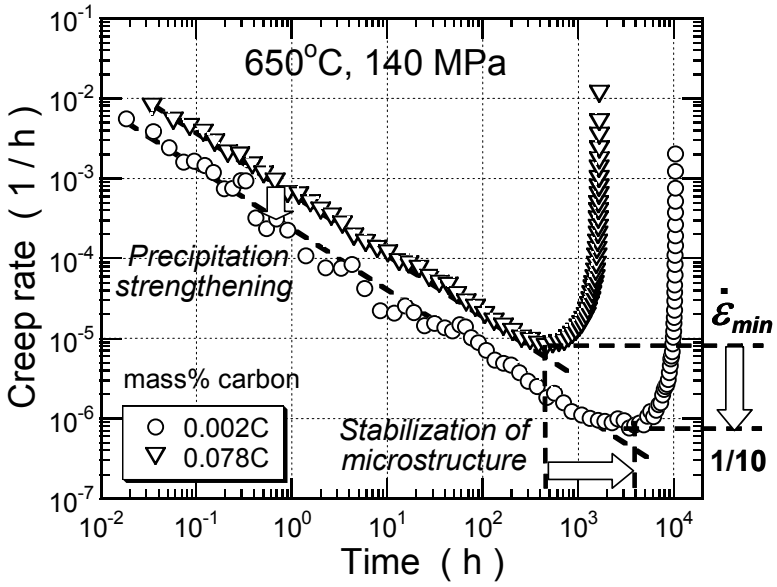

Figure 5 Creep rate versus time curves of 0.002C and 0.078C steels with 9Cr-3W-3Co-0.2V-0.05Nb base composition at 650°C and 140MPa [7].

Oxidation resistance in high-temperature steam

Figure 6 compares the weight gain due to oxidation in steam at 650 °C among the 9 to 12Cr steels [23]. The sheet specimens having a size of 10x20x2 mm were cut from bulk materials, which were already heat treated, ground on a SiC paper of 320 grit, rinsed in acetone and then supplied to the oxidation test in steam at 650°C. At present, we have no deciding criterion for oxidation resistance. We think that new steels for boiler components operating at 650°C should exhibit

oxidation resistance in steam at 650°C better than that of T91 and P91 in steam at 600°C, because T91 and P91 are being now used for long duration in power plants operating at 600°C. In Fig.6, the weight gain of T91 in steam at 600°C is shown by the dotted line. The weight gain of P92 (9Cr-0.5Mo-1.8W-VNb) and P122 (11Cr-0.4Mo-2W-CuVNb) in steam at 650°C is much larger than that of T91 at 600°C. This suggests that existing steels, even in 12Cr steel P122, cannot satisfy the present criterion for oxidation resistance in steam at 650°C. It should be noted that the weight gain of 9Cr-3WVNb steel with 3% Pd is significantly lower at 650°C than that of T91 at 600°C. Thin scale of Cr-rich oxide, presumably Cr_2O_3, forms on the specimen surface of 9Cr-3WVNb steel with 3%Pd in steam at 650°C, while thick scale consisting of magnetite in the outer layer and Fe-Cr spinel oxides in the inner layer forms on the surface of the other steels including T91. No evidence is found for the formation of Fe_3O_4 magnetite type oxide scale nor any oxide containing Pd in the 9Cr-3WVNb steel with 3%Pd. The TEM observations show that the surface grinding on a SiC paper produces strained region with a high density of dislocations about 1 μm beneath the specimen surface. The oxidation test of the 9Cr-3WVNb steel with 3%Pd after additional annealing at 750°C for 50 h in vacuum for strain release exhibits a large weight gain and the formation of thick scale

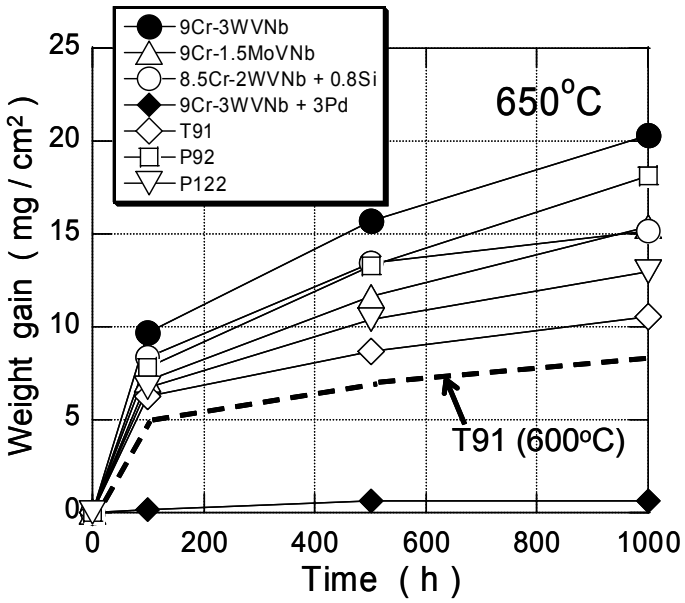

Figure 6 Weight gain of the steels in steam at 650°C as a function of time, comparing with that of T91 at 600°C shown by dotted line [23].

consisting of two layers similar as those in the other steels. The buff-polishing instead of the surface grinding on a SiC paper also exhibits a large weight gain and the formation of thick scale. The present results suggest that a combination of Pd addition and surface straining promotes the formation of protective Cr-rich oxide scale, which significantly improves the oxidation resistance in steam at 650 °C. It should be noted that the formation of protective Cr-rich oxide scale is a guiding principle for satisfying the oxidation resistance in steam at 650°C, although the addition of expensive Pd is economically not viable.

The formation of protective Cr-rich oxide scale is also achieved by a combination of Si addition and pre-oxidation treatment in argon gas at 700°C [24] and by a combination of shot-peening of Cr and pre-oxidation treatment in air at 700°C [25]. The oxidation test was carried out for 9Cr- 3WVNb steel containing different Si concentrations of 0 to 0.8% in steam at 650°C after pre-oxidation treatment in Ar gas. In the condition of no pre-oxidation treatment, the addition of Si decreases the weight gain of the steel in steam but the effect of Si is not large. The pre-oxidation treatment in Ar gas further decreases the weight gain during subsequent oxidation in steam. This is more

significant with increasing Si concentration and with increasing pre-oxidation time. The formation of thin scale of Cr-rich oxides is achieved by the addition of Si higher than 0.5% and by the pre-oxidation treatment in argon gas at 700°C for 20 h or more. The thin scale of Cr-rich oxides is stable during oxidation in steam at 650°C up to long times as shown in **Figure 7**, where the weight gain of 9Cr-3W-3Co-VNb-0.7Si-0.02B steel (MARB2; martensitic boron steel containing 200ppm boron) in steam at 650°C is shown as a function of time. Excellent oxidation resistance of MARB2 is also firmed even in the condition of no pre-oxidation by the Task 3 of EPRI project [26].

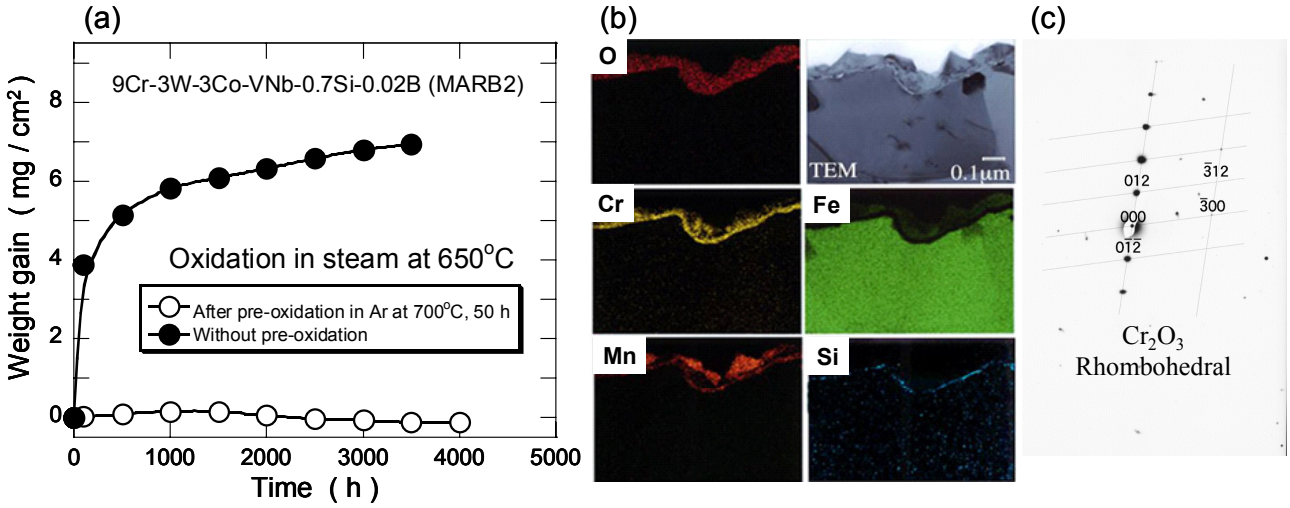

Figure 7 (a) Weight gain of 9Cr-3W-3Co-VNbSi steel (MARB2) in steam at 650°C, and (b) and (c) formation of protective Cr_2O_3 scale after pre-oxidation in argon at 700°C [24].

Exfoliation of thin scale of Cr-rich oxides, which formed during pre-oxidation treatment, has been investigated by cyclic oxidation test in steam. No evidence has been observed for the exfoliation of thin scale of Cr-rich oxides up to 40 cycles of cyclic heating and cooling in steam between 650 and 150°C. No difference is observed in weight gain between cyclic and continuous oxidation tests. Further investigation based on cyclic oxidation test under stress will be required.

Creep strength of welded joints

The creep rupture time of simulated HAZ specimens of P92 and P122 has its minimum after A_{C3} heating which produces fine-grained martensitic microstructure with high density of dislocations and enlarged $M_{23}C_6$ carbides but no lath structure [27-29]. The inhomogeneous recovery of excess dislocations and the coarsening of $M_{23}C_6$ are much more significant in the fine-grained A_{C3} simulated HAZ specimens during creep than in the A_{C1} simulated HAZ specimens and base metal. The onset of acceleration creep takes place at shorter times in the A_{C3} simulated HAZ specimens than in the A_{C1} simulated HAZ specimens and the base metal. This results in higher minimum creep rate and hence shorter time to rupture in the A_{C3} simulated HAZ specimens. The welded joints of P92 and P122 are fractured in fine-grained HAZ at low stresses, indicating Type IV fracture. Reducing the width of HAZ by EB welding is effective for the extension of creep life of welded joints, but the brittle Type IV fracture takes place at low stresses. Multi-axial stress condition in fine-grained HAZ with lower creep strength, resulting from mechanical constrain effect by the surrounding weld metal and base metal with higher creep strength, is essential for the formation of creep voids and brittle Type IV fracture in the fine-grained HAZ.

The addition of about 100ppm boron combined with minimized nitrogen as low as 10-20 ppm suppresses the Type IV fracture in HAZ at low stresses and improves the long-term creep rupture strength of welded joints [30, 31]. **Figure 8(a)** shows the creep rupture data for the welded joints of 130ppmB-9Cr steel and P92 at 650°C, comparing with those for their base metals. There is substantially no degradation of creep rupture strength in the 130ppmB-9Cr steel welded joints comparing with the base metal, while the degradation of creep rupture strength in P92 welded joints becomes more significant with increasing test duration. The observed degradation of creep rupture strength in P92 welded joints results from Type IV fracture. No degradation of creep rupture strength in welded joints was also observed for the 90ppmB-9Cr steel, similar as the 130ppmB-9Cr steel.

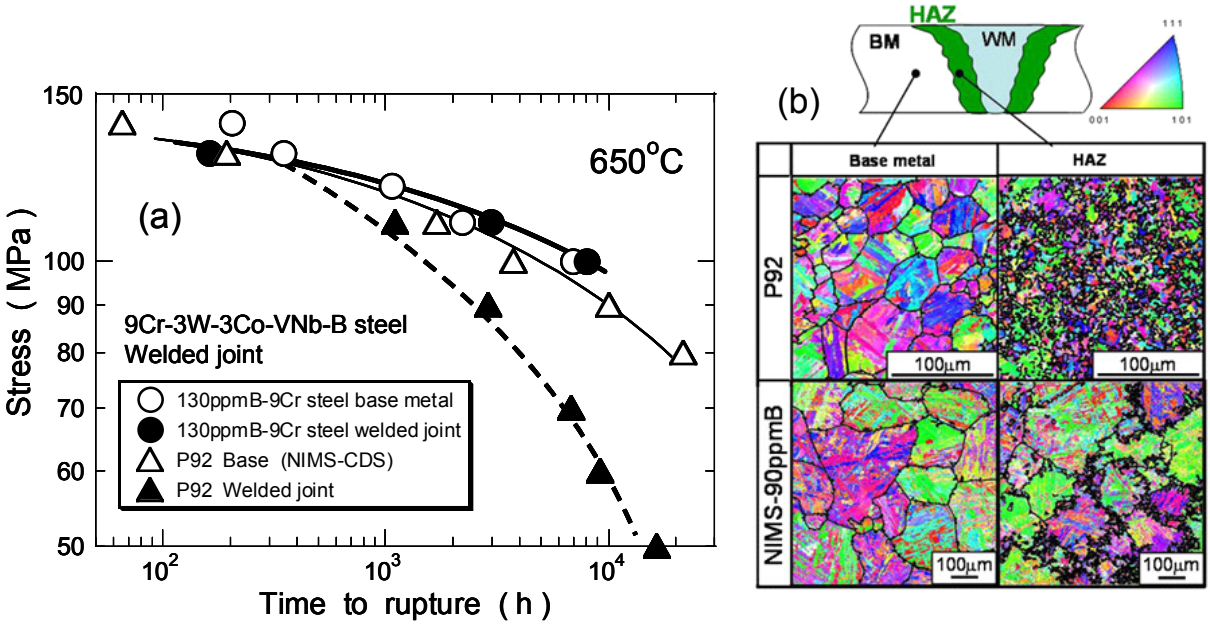

Figure 8 (a) Creep rupture data for welded joints of the 130ppmB-9Cr steel and P92 at 650°C and (b) microstructure of base metal and HAZ [30, 31].

Figure 8(b) shows the EBSP analysis of HAZ and base metal of the 90ppmB-9Cr steel and P92. Fine-grained microstructure, having average grain size of 10 μm or less, is observed to have formed in the A_{C3} heating HAZ of P92 welded joint. On the other hand, no evidence is observed for the formation of fine-grained HAZ in the 90ppmB-9Cr steel welded joints, which is also typical for the 130ppmB-9Cr steel welded joints. The average grain size is substantially the same between HAZ and base metal. Substantially no difference in microstructure between HAZ and base metal produces no mechanical constrain effect and hence no multi-axial condition in HAZ. This is a main reason responsible for the suppression of Type IV fracture by the addition of boron. There are two possibilities for the production of same grain size between HAZ and base metal in the boron steel. One of the possibilities is austenite memory effect, which has been shown to be a direct consequence of the existence of retained austenite in starting bainitic or martensitic microstructure [32, 33]. Another possibility is the effect of martensitic reverse transformation and suppression of subsequent recrystallization during austenitization in heat cycle of welding. Martensitic reverse transformation based on shear mechanism has been reported in 18%Ni maraging steel [34]. Grain boundary segregation of boron can reduce grain boundary energy, which suppresses nucleation of α/γ diffusive transformation at grain boundaries. Suppression of subsequent recrystallization can reproduce the same grain size as the original austenite. Further investigation will be required to

make clear the mechanisms responsible for the production of same grain structure between HAZ and base metal in the boron steel.
Although the addition of boron to 9Cr steel effectively suppresses Type IV fracture, the long-term creep rupture strength of base metal depends on boron content. Because upper limit of the creep strength of welded joints is provided by that of base metal, it is concluded that the increase in boron content improves the long term creep rupture strength of base metal and also welded joints of 9Cr steel without any degradation due to Type IV fracture.

HIGH STRENGTH AUSTENITIC STEELS

In the DOE Vision 21 project, two austenitic steels, HR6W (0.07C-23Cr-43Ni-6W-0.1Ti-0.2Nb) and Super 304H (0.1C-18Cr-9Ni-3Cu-NbN) are candidates for boiler tubing, while nickel base superalloys, such as Haynes 230, Inconel 740 and CCA 617, are candidates for both boiler tubing and piping [6]. In Japan, not only nickel base superalloys but also austenitic steel HR6W are considered as candidates for thick section steam lines of 700°C USC plant. Figure 9 shows the 10^5 h creep rupture strength for austenitic steels of HR6W, Super 304H and Alloy 800H, together with nickel base superalloys of Haynes 230, Inconel 740 and CCA 617, as a function of Larson-Miller parameter with a constant C = 20 [6]. On the upper side of figure, corresponding temperature is also shown. At 700°C, the 10^5 h creep rupture strength of HR6W is a little bit lower than 100 MPa, although it is approximately the same as that of standard 617 and larger than that of austenitic Super 304H and Alloy 800H.

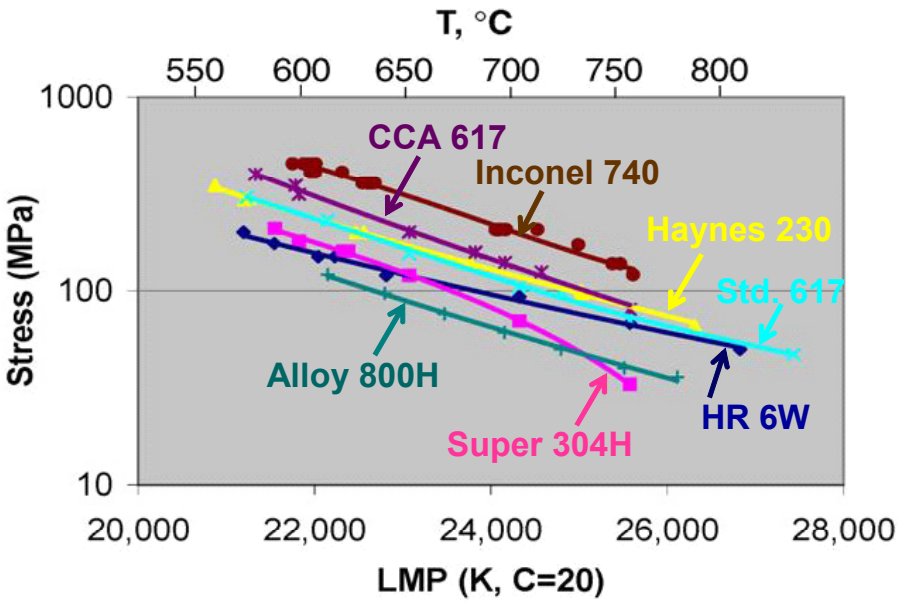

Figure 9 10^5 h creep rupture strength for several nickel base superalloys and austenitic steels as a function of Larson-Miller parameter with a constant C = 20 [6].

Igarashi et al. [35] pointed out that solution hardening by the elements such as Mo, W and N is essential for strengthening of austenitic alloys, while the phase stability against the σ embrittlement is required for long-term creep ductility and the resultant creep strength. These strengthening methods have successfully been used in HR6W. HR6W is strengthened by the combination of the dispersion of the precipitates such as $M_{23}C_6$, MX and fine Laves phase and the solid solution of W with the stabilization of the precipitates by B. This was confirmed by the TEM observations. To achieve further creep strengthening of HR6W for application to 700°C USC plant, the possibilities of increase in the amount of Laves phase and of introduction of γ' and α-Cr phases have been examined by phase diagram calculations. They also pointed out that in any case phase stability

against the σ phase formation is a key issue for achieving both high strength and enough ductility in austenitic steels.

CONCLUSIONS

1) The loss of creep strength in 9 to 12Cr steels at 550°C and above is shown to be mainly due to the dissolution of fine M_2X and MX carbonitrides during creep exposure, which is driven by the precipitation of coarse Z-phase and or M_6X carbonitrides which are thermodynamically more stable than the M_2X and MX. The sigmoidal inflection in creep rupture data can be predicted well by parametric analysis using Manson parameter.
2) Highly creep-resistant martensitic 9Cr steels strengthened by boron and by fine nitrides have been developed on the base of microstructure stabilization, especially in the vicinity of prior austenite grain boundaries. The new 9Cr steels exhibit higher creep rupture strength than existing high strength steels T91 and P92.
3) The formation of protective Cr-rich scale is achieved on the surface of 9Cr steel by the combination of Si addition and pre-oxidation treatment in argon gas at 700°C for 20 h or more. This significantly improves oxidation resistance of 9Cr steel in steam at 650°C.
4) The addition of boron suppresses the Type IV fracture in HAZ at low stresses and significantly improves the creep rupture strength of welded joints. No evidence is observed for the formation of fine-grained HAZ in the boron steel welded joints. Approximately no difference in microstructure between HAZ and base metal produces no mechanical constrain effect in HAZ.
5) At 700°C, the 10^5 h creep rupture strength of austenitic steel HR6W is a little bit lower than 100 MPa, although it is approximately the same as that of standard 617 and larger than that of austenitic Super 304H and Alloy 800H.

REFERENCES

1) K. Muramatsu, Advanced Heat Resistant Steel for Power Generation. The University Press, Cambridge, UK, (1999), p.543.
2) T.-U. Kern, K. Wieghthardt and H. Kirchner, Proc. 4th Int. Conf. on Advances in Materials Technology for Fossil Power Plants, Hilton Head Island, SC, USA (2004), CD-ROM.
3) F. Abe, Proc. 4th Int. Conf. on Advances in Materials Technology for Fossil Power Plants, Hilton Head Island, SC, USA (2004), CD-ROM.
4) B. Scarlin, T.-U. Kern and M. Staubli, Proc. 4th Int. Conf. on Advances in Materials Technology for Fossil Power Plants, Hilton Head Island, SC, USA (2004), CD-ROM.
5) R. Blum, R. W. Vanstone and C. Messelier-Gouze, Proc. 4th Int. Conf. on Advances in Materials Technology for Fossil Power Plants, Hilton Head Island, SC, USA (2004), CD-ROM.
6) R. Viswanathan, J. F. Henry, J. Tanzosh, G. Stanko, J. Shingledecker and B. Vitalis, Proc. 4th Int. Conf. on Advances in Materials Technology for Fossil Power Plants, Hilton Head Island, SC, USA (2004), CD-ROM.
7) F. Abe, Current Opinion in Solid State and Mater. Sci. 8, (2004), p.305.
8) V. Sklenicka, K. Kucharova, M. Svoboda, L. Kloc, J. Bursik and A. Kroupa, Mater. Character. 51 (2003), p.35.
9) H. Danielsen and J. Hald, Proc. 4th Int. Conf. on Advances in Materials Technology for Fossil Power Plants, Hilton Head Island, SC, USA (2004), CD-ROM.
10) H. Kushima, K. Kimura and F. Abe, Tetsu-to-Hagane, 85, (1999), p.841. (in Japanese)
11) A. Strang, V. Foldyna, J. Lenert, V. Vodarek and K.-H. Mayer, Proc. 6th Int. Charles Parsons Turbine Conf., Dublin, Ireland (2003), p.427.
12) K. Maruyama, E. Baba, K. Yokokawa, H. Kushima and K. Yagi, Tetsu-to-Hagane, 80, (1994),

p.336. (in Japanese)
13) K. Kimura, K. Sawada, K. Kubo and H. Kushima, ASME Pressure Vessel and Piping, 476, (2004), p.11.
14) N. Fujita, H. K. D. H. Bhadeshia, ISIJ Intern. 42, (2002), p.60.
15) Y. Murata, T. Koyama, M. Morinaga and T. Miyazaki, ISIJ Intern. 42, (2002), p.1423.
16) T. Horiuchi, M. Igarashi, F. Abe, K. Ohkubo, S. Miura and T. Mohri, Metall. Mater. Tran. A, 36A, (2005), in press.
17) F. Brun, T. Yoshida, D. J. Robsob, V. Narayan, H. K. D. H. Bhadeshia and D. J. C. MacKay, Mater. Sci. Technol. 15, (1999), p.547.
18) M. Taneike, F. Abe and K. Sawada, Nature, 424, (2003), p.294.
19) T. Horiuchi, M. Igarashi, F. Abe, ISIJ Intern. 42, (2002), p.S67.
20) S. Ukai and M. Fujiwara, J. Nucl. Mater. 307-311, (2002), p.749.
21) F. Abe, T. Horiuchi, M. Taneike, K. Sawada, Proc. 6th Int. Charles Parsons Turbine Conf., Dublin, Ireland (2003), p.379.
22) M. Staubli, B. Scarlin, K.-H. Mayer, T.-U. Kern, W. Bendick, P. Morris, A. DiGianfrancesco and H. Cerjak, Proc. 6th Int. Charles Parsons Turbine Conf., Dublin, Ireland (2003), p.305.
23) H. Kutsumi, T. Itagaki and F. Abe, Proc. 7th Liege Conf. on Mater. for Advanced Power Engineering 2002, Liege, Belgium, (2002), p.1629.
24) H. Kutsumi, H. Haruyama and F. Abe, Proc. 4th Int. Conf. on Advances in Materials Technology for Fossil Power Plants, Hilton Head Island, SC, USA (2004), CD-ROM.
25) H. Haruyama, H. Kutsumi, S. Kuroda and F. Abe, Proc. 4th Int. Conf. on Advances in Materials Technology for Fossil Power Plants, Hilton Head Island, SC, USA (2004), CD-ROM.
26) J. M. Sarver and J. M. Tanzosh, Proc. 4th Int. Conf. on Advances in Materials Technology for Fossil Power Plants, Hilton Head Island, SC, USA (2004), CD-ROM.
27) M. Tabuchi, T. Watanabe, K. Kubo, M. Matsui, J. Kinugawa and F. Abe, Int. J. Pressure Vessels & Piping 78, (2001), p.779.
28) M. Matsui, M. Tabuchi, T. Watanabe, K. Kubo, J. Kinugawa and F. Abe, ISIJ International, 41, (2001) S126-S130.
29) F. Abe and M. Tabuchi, Materials Science and Technology of Welding and Joining, 9, (2004) 22-30.
30) M. Kondo, S. K. Albert, M. Tabuchi, S. Tsukamoto, F. Yin, H. Okada and F. Abe, Proc. of 2nd Int. Conf. on Integrity of High Temperature Welds, London, UK, IOM Communications, (2003) p.123.
31) M. Tabuchi, M. Kondo, T. Watanabe, H. Hongo, F. Yin and F. Abe, Acta Metall. Sinica, 17, (2004), p.331.
32) S. T. Kimmins and D. J. Gooch : Metal Science, 17, (1983) 519-532
33) R. K. Shiue, K. C. Lan and C. Chen, Mater. Sci. Eng., A287, (2000) 10-16.
34) T. Maki, H. Morimoto and I. Tamura, Tetsu-To-Hagane, 65, (1979) 1598-1606. (in Japanese)
35) M. Igarashi, H. Semba and H. Okada, Proc. 8th Ultra-Steel Workshop, Tsukuba, Japan (2004), p.194.

HOME